

## Effect of Acid Extract of Leaves of *Juniperus procera* on Corrosion Inhibition of Carbon Steel in HCl Solutions

Ismat H. Ali, Mohamed H.A. Suleiman \*

Department of Chemistry, College of Science, King Khalid University, 9004Abha, Saudi Arabia

\*E-mail: [adamsuli67@hotmail.com](mailto:adamsuli67@hotmail.com)

Received: 20 August 2017 / Accepted: 22 January 2018 / Published: 6 March 2018

---

The efficiency of the hydrochloric acid leaf extract of *Juniperus procera* as a corrosion inhibitor against C-steel and its adsorption behavior were investigated in 1.0 M HCl solution using mass loss, potentiodynamic polarization, electrochemical impedance spectroscopy (EIS) techniques. Results revealed that the inhibition efficiency increased with the inhibitor concentration. EIS spectra exhibited one capacitive loop and confirmed the inhibitive capacity. The activation energy ( $E_a$ ) of the corrosion process clearly increased when the extract was used. The leaf extract was found to act as mixed-type inhibitor. The inhibition properties of the extract are discussed in terms of the mechanism by which its components adsorb onto the C-steel surface. This adsorption process obeyed a Langmuir adsorption isotherm.

---

**Keywords:** *Juniperus procera*. Corrosion, Inhibition, C-steel. EIS.

### 1. INTRODUCTION

Acids are used frequently in industrial sector for purposes such as, pickling, oil well acidification and cleaning of metals and alloys and ore production [1–3]. For this reason, there is an increase demand for new techniques to control and suppress corrosion which may be induced by using of these acids. Among these techniques, natural inhibitors have drawn attention as a cost-effective way for inhibiting acid corrosion [4–7]. Various organic compounds, such as acetylenic alcohol, quaternary ammonium salts and many other compounds that containing hetero atoms are extensively used as corrosion inhibitors in several industries. Organic molecules which have hetero atom such as O, S and N, are reported to be adsorbed on the surface of metals/alloy by blocking the active spots and creating a thin film and therefore reducing the passage of corrosive species to the metal/alloy surface [8–12]. There are numerous of factors affecting adsorption of constituents of natural products on the surface of metals or alloys (i) chemical structure of inhibitors (ii) charge of the metal (iii) nature of surface.

Compounds which are extracted from plants and have heterocyclic constituents, such as flavonoids, alkaloids and steroids proved effective corrosion inhibition properties, lack of irritating odor and excellent thermal stability [13–17]. Moreover these extracts are known to be eco-friendly and biodegradable materials.

*Juniperus procera* Hochst. ex Endl. (Cupressaceae), known locally as “Arar” is a tree often reaching 30-35 m high; widely distributed throughout the southern part of Saudi Arabia [18] and extends into Yemen and then across the Red Sea into Africa. Previous phytochemical study of different parts of *J. procera* resulted in the isolation of different classes of diterpenes, sesquiterpenes [19] and flavonoids [20].

The aim of this study was to investigate the efficiency of leaves extract of *J. procera* as a corrosion inhibitor for carbon steel in acidic aqueous solutions by using mass loss and electrochemical techniques.

## 2. EXPERIMENTAL

### 2.1. Material and medium

C-steel was used for all corrosion measurements. Its composition (wt %) is 0.22 C, 0.043 P, 0.35 Si, 0.48 Mn, 0.06 S, Fe balance. The aggressive solution (1.0 M HCl) was prepared by dilution of HCl (analytical grade, 37%) with bi-distilled water.

### 2.2. Extraction procedure

Leaves of *J. procera* were collected from Alsoda, Asir region, south of Saudi Arabia (during May 2017). Leaves were air-dried in the laboratory at room temperature and then grinded and defatted using petroleum ether and hexane. *J. procera* leaves extract (JPLE) was prepared by refluxing 500 grams of the defatted powder leaves for six hours in HCl solution (1.0 M). The extract was concentrated using an evaporator and then dried on a steam bath until a solid residue is obtained. The required concentrations of JPLE were prepared by dissolving the appropriate weight (0.5, 1.0, 1.5, 2.0 and 2.5) g of the solid residue in 1 L of HCl (1.0 M) for mass loss and electrochemical measurements. Another quantity of leaves powder (300 g) was macerated in ethanol (70%, 3 x 1 L) for 48 hours. The obtained extracts were filtered, combined and concentrated to dryness using rotary evaporator. The residue (78 g) was dissolved in methanol (80%, 500 mL) and defatted by shaking with petroleum ether (3 x 300 mL). The 80% aqueous methanol fraction yielded 35 g residue after evaporation to dryness.

### 2.3. Preliminary phytochemical screening

Phytochemical tests were performed to identify the classes of phytochemical constituents present in the ethanol leaf extract. The standard qualitative phytochemical procedures described by Trease and Evans [21], and Harborne [22] were adopted.

#### 2.4. Determination of total phenolic content

The total phenol content of the methanol fraction was determined using the Folin-Ciocalteu method as described by Salgueiro et al. [23] and Adedapo et al. [24], with slight modification. The absorbance of blue-colored mixture was measured at 760 nm using UV-Vis spectrophotometer. Gallic acid was used for constructing the standard curve. The amount of total phenol content was expressed as mg gallic acid equivalent (GAE) /g of extract.

#### 2.5. Determination of total flavonoid content

The total flavonoid content was estimated using the Aluminium chloride method as described by Adedapo et al. [24] and Meda et al. [25], with minor modification. Briefly, 2 mL of a 2%  $\text{AlCl}_3$  methanolic solution was added to same volume of plant extract (2.0 mg/mL in methanol). After 30 min of incubation at room temperature, the absorbance values were measured at 415 nm against a methanol blank. The total flavonoid content, expressed as milligrams of quercetin equivalent per gram of extract (mg QE /g), was calculated using a calibration curve prepared with quercetin that was analyzed in the same manner as the extracts. The calculations were performed in triplicate.

#### 2.6. Mass loss experiments

The mass loss of the C-steel coupons of 5.0 \* 2.5 \* 0.2 cm dimensions in 1.0 M HCl solutions in the absence and existence of different concentrations of the inhibitor was determined at 25° C. Prior to each experiment, the C-steel surface was abraded with different sizes of emery papers, then cleaned in ultrasonic bath with ethanol and acetone, and finally washed with bi-distilled water and dried. After weighing accurately, the specimens were immersed in 150 ml of the corrosive acidic solution for six hours. Then, the specimens were taken out, cleaned, dried and reweighed. The experiments were done in triplicate to ensure the reproducibility of results. The average value of the mass loss was calculated. Mass loss experiments were performed at different temperatures as well in order to estimate some thermodynamic parameters.

#### 2.7. Electrochemical measurements

Electrochemical measurements were performed in a cell contains three electrodes assembly using Autolab model PGSTAT30 potentiostat/galvanostat, controlled by GPES/FRA electrochemical software. In addition to the working electrode; a saturated calomel electrode (SCE) and platinum electrode which were used as reference and counter electrodes, respectively. The working electrodes were 0.8 cm diameter and were welded from one side to a copper wire used for electrical connection. The electrodes were abraded with different grades of emery paper, degreased with acetone, rinsed with bi-distilled water and dried between filter papers. All experiments were performed at  $25.0 \pm 0.1$  °C.

The Tafel potentiodynamic curves were recorded from -500 to +500 mV at a scan rate of 1.0 mV s<sup>-1</sup> after a steady state of 30 minutes.

Electrochemical impedance spectroscopy (EIS) was carried out using the same instrument. The EIS measurements were recorded at the frequency range of 50 mHz to 0.01 mHz. EIS data were analyzed with FRA software with amplitude of 5 mV peak-to-peak using ac signals at respective corrosion potential. Polarization resistance (Rp) and constant phase element (CPE) were obtained from Nyquist plots.

### 3. RESULTS AND DISCUSSION

#### 3.1. Characterization of *J. procera* leaf extract

The phytochemical screening of ethanol extract of *J. procera* leaves revealed the presence of flavonoids, tannins, triterpenes, alkaloids and saponins. Some of these phytochemical constituents have already been reported in methanolic leaves extract of this plant [26]. Isolation of flavonoids from leaves extract of *J. procera* was reported by Mujwah et al. [27]. Mossa et al. [28] isolated terpenoids, phenolic diterpene and organic acid from leaves and barks of *J. procera*. The total phenolic content of leaf methanol fraction was estimated by using Folin–Ciocalteu reagent. Total phenolic content of *J. procera* leaves extract was reported as gallic acid equivalents and found to be 131.06 ± 0.14 mg (GAE)/g dry extract. The total flavonoid content was found to be 49.21 ± 0.39 mg, expressed as quercetin equivalents per gram of extract (mg QE/g). These results are in agree with that reported by Samaha et al. [29]. Flavonoids have been reported to be present in effective green corrosion inhibitors [30-32]. The corrosion inhibition activity of flavonoids could be due to presence of electron rich multiple bonds and heteroatoms [33,34].

#### 3.2. Mass loss method

The corrosion behavior of C-steel in 1.0 M HCl solutions with and without various concentrations of *J. procera* extract was examined at 298 K. Table 1 gives values of the rate of corrosion (mg /cm<sup>2</sup> h), inhibition efficiency (E %) for corrosion of C-steel and values of surface coverage Θ.

The gravimetric results show that the corrosion rate was suppressed gradually with increasing extract concentration. The mass loss data were used to determine inhibition efficiency (IE%) and using equations 1:

$$IE\% = \frac{w_o - w_i}{w_o} \times 100 \quad (1)$$

Where  $w_i$  and  $w_o$  are the mass losses in the presence and absence of extract respectively. It is obvious that 2.5 g/L of the extract concentration serves as an optimum concentration that achieves the highest efficiency of corrosion inhibition. An increase of inhibitor concentration beyond 2.5 g/L resulted in a diminished corrosion protection. Table 1 also shows that the extract can protect C-steel against acid corrosion at room temperature. This result is due to fact that the coverage of carbon steel

surface by the extract constituents increases with inhibitor concentrations. This behavior indicates that the C-steel surface is effectively isolated from the corrosive medium by the inhibitor adsorption film [35].

**Table 1.** Gravimetric results of the C-steel corrosion with and without addition of **JPLE** after 6 hours of immersion in 1.0 M HCl at 298 K.

Conc. (g/L)	W (mg/cm <sup>2</sup> .h)	EI%	Θ
blank	0.1487	-	-
0.50	0.0829	44.3	0.443
1.0	0.0561	62.2	0.622
1.5	0.0431	71.0	0.710
2.0	0.0339	77.1	0.673
2.5	0.0206	86.0	0.860

### 3.3. Potentiodynamic polarization measurements

Some kinetic properties of the cathodic and anodic reactions have been determined through measurements of polarization curves. The polarization behavior of C-steel electrode in 1.0 M HCl solutions is presented in Fig. 1 in the absence and existence of several concentrations of HCl solution. It is obvious from Fig. 1 that both anodic and cathodic reactions are influenced by the inhibitor. It also clear that the inhibition efficiency increases as the inhibitor concentration increases, meaning that the addition of the inhibitor reduces the anodic dissolution of C-steel and also hinders the cathodic reactions. Therefore, the investigated inhibitor can be classified as mixed type inhibitor.

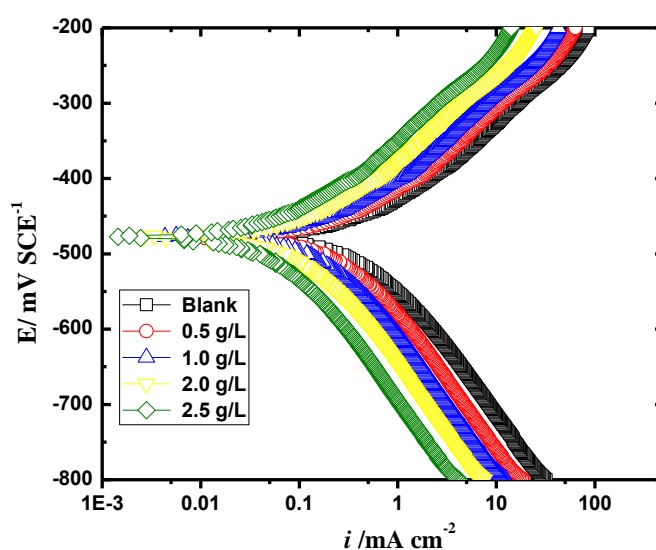


**Figure 1.** Tafel polarization curves for the corrosion of C-steel in 1.0 M HCl in the absence and presence of various concentrations of at  $25.0 \pm 0.1$  °C.

Kinetic parameters such as corrosion current densities ( $i_{\text{corr}}$ ), corrosion potential ( $E_{\text{corr}}$ ),

cathodic Tafel slope ( $\beta_c$ ), anodic Tafel slope ( $\beta_a$ ) and inhibition efficiency (% IE) were calculated from the curves of Fig. 1 and are listed in Table 2. These results revealed that the corrosion current density decreases noticeably after the addition of inhibitor in 1.0 M HCl and % IE increases with increasing the inhibitor concentration. IE% of JPLE is equal or higher than those achieved by other natural products inhibitors [9, 10]. In the presence of inhibitors  $E_{\text{corr}}$  was enhanced with no definite trend, indicating that the inhibitor acts as mixed-type inhibitors. The inhibition efficiency was calculated using equation (2):

$$\%IE_p = [(i_{\text{corr}}^0 - i_{\text{corr}})/i_{\text{corr}}^0] \times 100 \quad (2)$$

Where  $i_{\text{corr}}^0$  and  $i_{\text{corr}}$  are the uninhibited and inhibited corrosion current densities, respectively.

**Table 2.** Effect of concentrations of **JPLE** on some kinetic parameters for C-steel in 1.0 M of HCl at  $25 \pm 0.1$  °C.

Conc. (g/L)	- $E_{\text{corr}}$ (mV vs. SCE)	$i_{\text{corr}}$ ( $\mu\text{A cm}^{-2}$ )	- $\beta_a$ (mV dec <sup>-1</sup> )	$\beta_c$ (mV dec <sup>-1</sup> )	% IE
Blank	485	254.8	48	139	-----
0.50	465	123.5	62	148	51.5%
1.0	471	95.8	91	151	62.4
2.0	460	73.3	78	158	71.2
2.5	477	28.3	97	143	88.8

Results in Table 2 indicate that the slopes of the anodic ( $\beta_a$ ) and cathodic ( $\beta_c$ ) Tafel lines remain almost unchanged upon addition of the inhibitor, giving rise to a nearly parallel set of anodic lines, and almost parallel cathodic plots results too. Thus the adsorbed inhibitors act by simple blocking of the active sites for both anodic and cathodic processes. i. e. the adsorbed inhibitor decreases the surface area for corrosion without affecting the corrosion mechanism of C-steel and only causes inactivation of a part of the surface with respect to the corrosive medium [36, 37].

#### 3.4. Electrochemical impedance spectroscopy (EIS)

EIS is a firm and powerful method in corrosion studies. A lot of data such as, kinetic parameters, surface properties, and mechanistic information can be deduced from impedance diagrams [38-41]. Fig. 2 shows Nyquist plots obtained at open-circuit potential in the existence and absence of various concentrations of investigated extract at  $25.0 \pm 0.1$  °C.

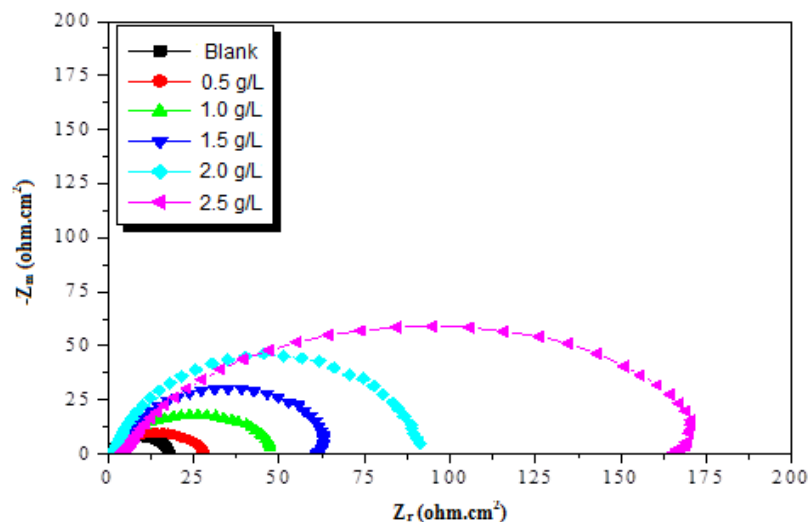


**Figure 2.** EIS Nyquist plots for C-steel surface in 1.0 M HCl in the absence and presence of different concentrations of JPLe 25 ± 0.1 °C.

Results show that the capacitive loop size increases gradually as the extract concentration increases indicating that a barrier is formed on the C-steel surface. The Nyquist plots do not exhibit ideal semicircles. The deviation from perfect semicircle may be ascribed to the frequency dispersion [42] as well as to the surface heterogeneity. The double layer capacitance,  $C_{dl}$ , was determined from equation (3):

$$C_{dl} = Y_o \omega^{n-1} / \sin [n (\pi/2)] \tag{3}$$

Where  $Y_o$  is the magnitude of the CPE,  $\omega = 2\pi f_{max}$ ,  $f_{max}$  is the maximum frequency of the imaginary component of the impedance and the factor  $n$  is an adjustable parameter that usually lies between 0.50 and 1.0.

It can be deduced from the Nyquist plots, that the curves approximated by a single capacitive semicircles, showing that the corrosion process was mainly charged-transfer controlled [43-45]. All samples have identical shapes (in existence and absence of inhibitor at various immersion times) proving that no change in the corrosion mechanism [46].

**Table 3.** Electrochemical kinetic parameters obtained by EIS technique for C-steel in 1.0 M HCl without and with various concentrations **JPLe** at 25 ± 0.1 °C.

Conc. (g/L)	$Y_o \times 10^{-3}$	n	$R_{ct}$ ( $\Omega$ cm <sup>2</sup> )	$C_{dl} \times 10^{-3}$ ( $\mu$ Fcm <sup>-2</sup> )	%IE
Blank	112.4	0.89	42.6	87.6	-
0.5	91.5	0.78	96.6	40.0	55.9
1.0	73.8	0.81	114.3	31.4	62.7
1.5	57.7	0.82	154.7	23.3	72.5
2.0	35.1	0.85	195.6	15.1	78.2
2.5	21.2	0.86	298.8	9.7	85.7

From Table 3, it is concluded that  $R_{ct}$  value increases with increasing the extract concentration and in turn % IE increases, which is in a good agreement with the Polarization results. The decrease in  $CPE/C_{dl}$  values is attributed to a decrease in local dielectric constant and/or an increase in the thickness of the double layer, suggesting that the extract inhibits the C-steel corrosion by adsorption at metal/acid interphase [47, 48]. Values of inhibition effectiveness were calculated from the charge transfer resistance data using equation (4) [49]:

$$\% IE_{EIS} = [1 - (R_{ct}^{\circ} / R_{ct})] \times 100 \tag{4}$$

Where  $R_{ct}$  and  $R_{ct}^{\circ}$  are the charge-transfer resistance values with and without inhibitor, respectively.

### 3.5. Adsorption isotherm

Adsorption isotherm models give important information on the interaction between the inhibitor molecules and the metal surface. The  $\theta$  values obtained from gravimetric technique have been used to explain the best isotherm that describes the adsorption process. In order to determine the best adsorption isotherm, which define the adsorption of the extract on the C-steel surface, a number of adsorption isotherm models such as, Langmuir, Freundlich and Temkin, have been verified. However, the convenient model was found to be Langmuir which is described by Equation (5)

$$C_{inh}/\theta = 1/K_{ads} + C_{inh} \tag{5}$$

Where  $C_{inh}$  stands for inhibitor concentration,  $\theta$  is the surface coverage and  $K_{ads}$  is the adsorption equilibrium constant.

Free energy change of adsorption  $\Delta G_{ads}$  is calculated by equation (6)

$$\Delta G_{ads} = -RT \ln 55.5 K_{ads} \tag{6}$$

Where T is the absolute temperature and R is the universal gas constant. Fig. 5 confirms that the adsorption behavior of the inhibitor obeys Langmuir model.  $\Delta G_{ads}$  value was determined as -11.1 kJ/mole indicating that the adsorption of the extract is a physio-sorption and spontaneous process [40].

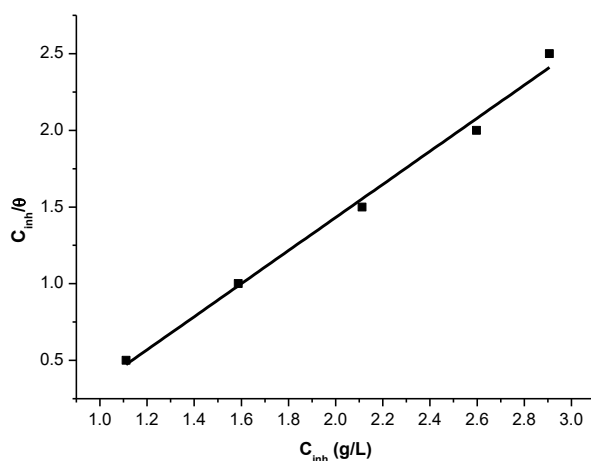


**Figure 3.** Plots of Langmuir adsorption isotherm of JPLe on the C- steel surface at 298 K.



### 3.6. Effect of temperature

The influence of temperature on the inhibited system is usually complicated. This is attributed to (i) the fast desorption and (ii) possible decomposition of the inhibitor. In order to determine some thermodynamic parameters, mass loss measurements were carried out at temperature range 25 – 55°C in the presence and absence of JPLe.

**Table 4.** Effect of temperature on corrosion behavior of C-steel without and with 1.5 g/L of JPLe

	Temperature (°C)	C <sub>R</sub> (mg/cm <sup>2</sup> .h)	EI%
Blank	25.0	1.487	-
	35.0	1.893	-
	45.0	2.398	-
	55.0	3.087	-
JPLe	25.0	0.431	44.3
	35.0	0.561	62.2
	45.0	0.691	71.0
	55.0	0.839	77.1

Results shown in Table 4 revealed that the corrosion rate increases with temperature both in inhibited and uninhibited systems. Arrhenius equation which is represented by equation 7 is used to calculate the activation energy, while Eyring equation, which is represented by equation 8, is used to determine enthalpy and entropy of activation. Values of the activation parameters are shown in Table 5.

$$\ln C_R = \frac{-E_a}{RT} + \ln A \quad (7)$$

$$\ln \frac{C_R}{T} = \frac{\Delta S^*}{RT} + \ln \frac{k_B}{h} + \frac{\Delta H^*}{R} \quad (8)$$

where C<sub>R</sub> is corrosion rate, E<sub>a</sub> is the activation energy, A is the frequency factor, T is the absolute temperature, ΔH\* is the enthalpy change of activation, ΔS\* is the entropy change of activation, R is the universal gas constant, h is Planck's constant and k<sub>B</sub> is the Boltzmann constant.

Results obtained from slope of Figure 4 and Table 4, revealed that E<sub>a</sub> increases in the existence of JPLe proving that the corrosion rate decreases. Values of ΔH\* and ΔS\* are calculated from slope and intercept of Figure 5 and equation 8, respectively.

**Table 5.** Values of some activation parameters of the corrosion process of C-steel in 1.0 M HCl in the absence and presence of JPLe

system	E <sub>a</sub> (kJ/mol)	ΔH* (kJ/mol)	ΔS* (J/mol.K)
Blank	17.2	14.4	-197.6
JPLe	25.4	22.6	-182.4

The negative values of entropy of activation ( $\Delta S^*$ ) imply that the activated complex throughout the rate-determining step is an association rather than a dissociation step [51], indicating that a decrease in disordering occurs on going from reactants to the activated complex [52,53]. The negative signs of  $\Delta H^*$  indicates that the corrosion process is an endothermic.

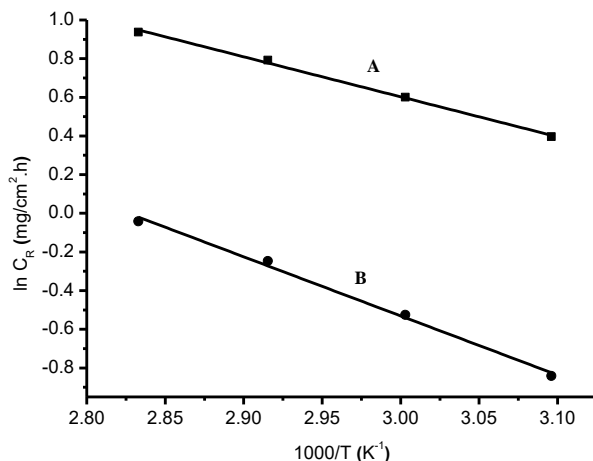


**Figure 4.** Arrhenius plot of the corrosion process of C-steel without (A) and with (B) JPLe

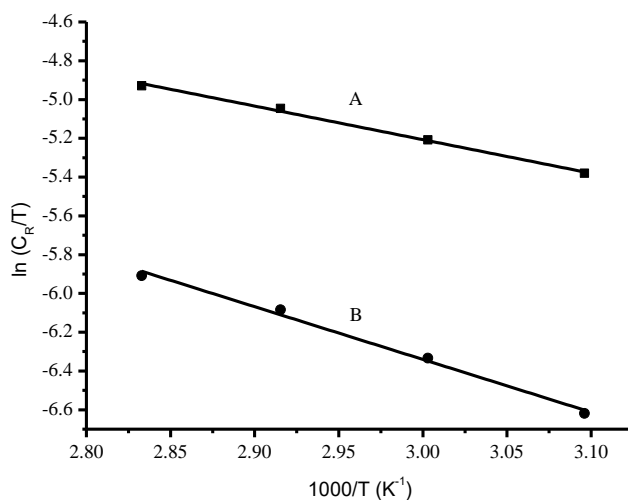


**Figure 5.** Eyring plot of the corrosion process of C-steel without (A) and with (B) JPLe

### 3.6 Comparison of JPLe with other extracts

Comparison of the maximum inhibition efficiency, IE%, of JPLe with those of some other plant extracts stated in the literature is given in Table 6. Variances in IE% could be ascribed to the properties and nature of each extract such as structure and surface area.

**Table 6.** Comparison of maximum inhibition effect (IE%) for different extracts of plants

Plant type	Maximum IE%
<i>Trigonella foenum-graecum L Seeds</i> [54]	91.8
<i>Psidium Guajava Seeds</i> [55]	81.2
<i>Khaya senegalensis leaves</i> [56]	89.0
<i>Junipers leaves</i> [57]	90.3
<i>Capparis spinosa leaves</i> [58]	87.6
<i>This study</i>	87.2

Data in Table 6 prove that the efficiency of the leaves extract of *J. procera* is a promising corrosion inhibitor. Defatting prior to extraction may increase its efficiency.

#### 4. CONCLUSION

This study proves that *J. procera* extract have good ability to inhibit the corrosion of C- steel in 1.0 M HCl. Results obtained from mass loss, DC polarization, and AC impedance methods are reasonably in fair agreement and confirmed that the inhibitor efficiency increases with increasing inhibitor concentration. It has been proved that the *J. procera* extract acts as mixed-type inhibitor. The results of EIS revealed that an increase in the charge transfer resistance and a decrease in double layer capacitances when the inhibitor is added and hence an increase in % IE. This is attributed to increase of the thickness of the electrical double layer.

#### ACKNOWLEDGEMENTS

The authors extend their appreciation to the Deanship of Scientific Research at King Khalid University for funding this work through General Research Project under grant number (G.R.P- 270 -38)

#### References

1. M.E. Mashuga, L.O. Olasunkanmi and E.E. Ebenso, *J. Mol. Struct.*, 1136 (2017) 127.
2. F. Bentiss, M. Lebrini, H. Vezin and M. Lagrenee, *Mater. Chem. Phys.*, 87 (2004) 18.
3. X. Liu, P.C. Okafor and Y.G. Zheng, *Corros. Sci.*, 51 (2009) 744.
4. H. Lgaz, K. S. Bhat, R. Salghi, Shubhalaxmi, S. Jodeh, M. Algarra, B. Hammouti, I. H. Ali and A. Essamri, *Journal of Molecular Liquids*, 238 (2017) 71.
5. O. El Mouden, A. Anejjar, M. Messali, R. Salghi, H. A. Ismat and B. Hammouti, *Chem. Sci. Rev Lett.*, 3 (2014) 579.
6. I. H. Ali and M. I. Khan, *Int. J. Electrochem. Sci.*, 12 (2017) 2285.
7. N. S. Patel, J. Hadlicka, P. Beranek, R. Salghi, H. Bouya, H. A. Ismat and B. Hammouti, *Portugaliae Electrochimica Acta*, 32 (2014) 395.
8. A.S. Fouda, K. Shalabi and H. Elmogazy, *J. Mater. Environ. Sci.*, 5 (2014) 1691.

9. M.J. Bahrami, S.M.A. Hosseinia and P. Pilvar, *Corros. Sci.*, 52 (2010) 2793.
10. M.M. Solomon, S.A. Umoren, I.I. Udoso and A.P. Udoh, *Corros. Sci.*, 52 (2010) 1317.
11. F.G. Liu, M. Du, J. Zhang and M. Qiu, *Corros. Sci.*, 51 (2009) 102.
12. A.Y. Musa, A.A.H. Kadhum, A.B. Mohamad and M.S. Takriff, *Corros. Sci.*, 52 (2010) 3331.
13. K.F. Khaled and M.A. Amin, *Corros. Sci.*, 51 (2009) 1964.
14. P. Kumar and A. N. Shetty, *Res. Chem. Intermed.*, 41 (2015) 7095.
15. H. B. Ouici, O. Benali and A. Guendouzi, *Res. Chem. Intermed.*, 42 (2016) 7085.
16. K. F. Al-Azawi, S. B. Al-Baghdadi and A. Z. Mohamed, *Chem. Cent. J.*, 10 (2016) 23.
17. M. Yadav, D. Behera and U. Sharma, *Arab. J. Chem.*, 9 (2016) 1487.
18. A. A. Mujwah, M. A. Mohammed and M. H. Ahmed, *Arab. J. Chem.*, 3 (2010) 85.
19. S. I. Alqasoumi and M. S. and Abdel-Kader, *Pak. J. Pharm. Sci.*, 25 (2012) 315.
20. I. Muhammad, J. S. Mossa and F. S. El-Fery, *Phytother. Res.*, 10 (1996) 604607.
21. G. E. Trease and W. C. Evans, (1989). *Pharmacognosy*. 13th edition. English Language Book Society, Bailliere Tindall, Britain, London.
22. J. B. Harborne, (1998). *Phytochemical Methods: A Guide to Modern Techniques of Plant Analysis*. 3rd edition. Springer, UK.
23. F. B. Salueiro, A. F. Lira, V. M. Rumjanek and R. N. Castro, *Quim. Nova*, 37 (2014) 821.
24. A. A. Adedapo, F. O. Jimoh, S. Koduru, P. J. Masika and A. J. Afolayan, *BMC Complement Altern. Med.*, 9(2009) 21.
25. A. Meda, C. E. Lamien, M. Romito, J. Millogo and O. G. Nacoulma, *Food Chem.*, 91 (2005) 571.
26. A. A. Ali, and M. N. Elgimabi, *Int. J. Chem. Sci.*, 13 (2015) 1883.
27. A. A. Mujwah, M. A. Mohammed and M. H. Ahmed, *Arabian Journal of Chemistry*, 3 (2010) 85. doi:10.1016/j.arabjc.2010.02.003.
28. J. S. Mossa, F. S. El-Fery and I. Muhammad, *Phytother. Res.*, 18 (2004) 934.
29. H. A. M. Samaha, N. A. A. Ali, I. Mansi and R. Abu-El-Halawa, *World Journal of Pharmacy and Pharmaceutical Sciences*, 6 (2017) 232.
30. J.C. Rocha, J.A. Cunha, P. Gomes and E.D. Elia, *Mater. Res.*, 17 (2014) 1581.
31. M. Shyamala and P. K. Kasthuri, *Int. J. Corros.*, 8 (2012) 1.
32. I. Ikeuba, B. I. Ita, P. C. Okafor, B. U. Ugi and E. B. Kporokpo, *Prot Met Phys Chem. Surf.*, 51 (2015) 1043.
33. P. B. Raja and M. G. Sethuraman, *Materials Letters*, 62 (2008) 113.
34. N. O. Eddy, *Port. Electrochim. Acta*, 27 (2009) 579.
35. K. Hu, J. Zhuang, J. Ding, Z. Ma, F. Wang and X. Zeng, *Corros. Sci.*, 125, (2017) 68.
36. M.A. Al-Khaldi and K.Y. Al-qahtani, *J. Mater. Environ. Sci.*, 4 (2013) 593.
37. J.W. Schltze and K. Wippermann, *Electrochim. Acta*, 32 (1987) 823
38. D.C. Silverman and J.E. Carrico, *Corrosion*, 44 (1988) 280.
39. D.D. Macdonald and M.C.H. Mckubre, "Impedance measurements in electrochemical systems" *Modern Aspects of Electrochemistry*, J.O'M. Bockris, B.E. Conway, R.E. White, Eds., Plenum Press, New York . 14 (1982 ) 61.
40. F. Mansfeld, *Corrosion*, 36 (1981) 301.
41. C. Gabrielli, "Identification of Electrochemical processes by Frequency Response Analysis" Solarton Instrumentation Group, 1980.
42. S.F. Mertens, C. Xhoffer, B.C. Decooman and E. Temmerman, *Corrosion*, 53 (1997) 381.
43. G. Trabaneli, C. Montecelli, V. Grassi and A. Frignani, *J. Cem. Concr. Res.*, 35 (2005) 1804.
44. A.J. Trowsdate, B. Noble, S.J. Haris, I.S.R. Gibbins, G.E. Thomson and G.C. Wood, *Corros. Sci.*, 38 (1996) 177.
45. F.m. Reis, H.G. de Melo and I. Costa, *J. Electrochem. Acta*, 51 (2006) 1780.
46. M. Lagrenée, B. Mernari, M. Bouanis, M. Traisnel, F. Bentiss, *Corros. Sci.*, 44 (2002) 573.
47. E. McCafferty and N. Hackerman, *J. Electrochem. Soc.*, 119 (1972) 999.
48. H. Ma, S. Chen, L. Niu, S. Zhao, S. Li and D. Li, *J. Appl. Electrochem.*, 32 (2002) 65.

49. E. Kuş and F. Mansfeld, *Corros. Sci.*, 48 (2006) 965.
50. I. H. Ali and H. A. Alrafai, *Chemistry Central Journal*, 10 (2016) 36.
51. I. H. Ali and Y. Sulfab, *Int. J. Chem. Kinet.*, 43 (2011) 563.
52. I. H. Ali and Y. Sulfab, *Int. J. Chem. Kinet.*, 44 (2012) 729.
53. R. Salghi, S. Jodeh, Eno E. Ebenso, H. Lgaz, D. Ben Hmamou, I. H. Ali , M. Messali, B. Hammouti and N. Benchat, *Int. J. Electrochem. Sci.*, 12 (2017) 3309.
54. A. Ennouri, A. Lamiri and M. Essahli, *Portugaliae Electrochimica Acta*, 35 (2017) 279.
55. Y. C. Sharma and S. Sharma, *Portugaliae Electrochimica Acta*, 34 (2016) 365.
56. I. H. Ali, *Int. J. Electrochem. Sci.*, 11 (2016) 2130.
57. L. Bammou, R. Salghi, A. Zarrouk, H. Zarrok, S. S. Al-Deyab, B. Hammouti, M. Zougagh and M. Errami, *Int. J. Electrochem. Sci.*, 7 (2012) 8974.
58. F. Wedian, M. A. Al-Qudaha and A. N. Abu-Bakerb, *Portugaliae Electrochimica Acta*, 34(2016) 39.

© 2018 The Authors. Published by ESG ([www.electrochemsci.org](http://www.electrochemsci.org)). This article is an open access article distributed under the terms and conditions of the Creative Commons Attribution license (<http://creativecommons.org/licenses/by/4.0/>).